

# Synthesis and characterization of polybenzoxazine networks nanocomposites containing multifunctional polyhedral oligomeric silsesquioxane (POSS)

Yuan-Jyh Lee, Shiao-Wei Kuo <sup>\*</sup>, Chih-Feng Huang, Feng-Chih Chang <sup>\*</sup>

*Institute of Applied Chemistry, National Chiao-Tung University, Hsin-Chu, Taiwan, ROC*

Received 2 November 2005; received in revised form 8 March 2006; accepted 27 March 2006

Available online 6 May 2006

## Abstract

A new class of polybenzoxazine/POSS nanocomposites with network structure is prepared by reacting multifunctional benzoxazine POSS (MBZ-POSS) with benzoxazine monomers (Pa and Ba) at various compositional ratios. Octafunctional cubic silsesquioxane (MBZ-POSS) is used as a curing agent, which is synthesized from eight organic benzoxazine tethers through hydrosilylation of vinyl-terminated benzoxazine monomer (VP-a) with octakis(dimethylsiloxy)silsesquioxane ( $Q_8M_8^H$ ) using a platinum complex catalyst (Pt-dvs). Incorporation of the silsesquioxane core into polybenzoxazine matrix could significantly hinder the mobility of polymer chains and enhance the thermal stability of these hybrid materials. For these nanocomposites, increasing the POSS content in the hybrids is expected to improve its thermal properties with respect to the neat polybenzoxazine. The morphology feature is useful to explain the thermal property changes ( $T_g$  and  $T_d$ ) and AFM images show that the presence of POSS aggregation in larger scales occurs at higher POSS contents. The reason of the heterogeneous phase separation may be from the less compatibility of the inorganic silsesquioxane core with organic benzoxazine species and the homopolymerization of MBZ-POSS. In the course of the formation of the polybenzoxazine/POSS hybrids, POSS particles were separated from the polybenzoxazine rich region, leading to POSS rich domains in the range of 50–1000 nm.

© 2006 Elsevier Ltd. All rights reserved.

*Keywords:* POSS; Benzoxazine; Thermal property

## 1. Introduction

Polybenzoxazine is a newly developed thermoset resin. Benzoxazine monomers are heterocyclic compounds featuring an oxazine ring and are synthesized by the reaction between a primary amine, phenol, and formaldehyde. Benzoxazine monomers can be polymerized by ring-opening polymerization in the absence of a catalyst and releases no byproduct [1,2]. Furthermore, polybenzoxazine has unique properties not found in traditional phenolic resins such as excellent dimensional stability, flame retardance, stable dielectric constant, and low moisture absorption [3–5]. To further improve the performance of polybenzoxazines, the polymerizable acetylene side groups have been introduced into the benzoxazine monomer [6–9]. The acetylene-functional benzoxazine can be polymerized into three dimensional networks products showing improved high thermal and mechanical stability, high solvent and moisture

resistances. Another approach to improve the stability of polybenzoxazines is by blending with other polymers [10–13], such as poly(imide-siloxane), polyurethane, epoxy resin or incorporating clay [14,15] into the polybenzoxazine matrix.

The development of polymer–inorganic nanocomposites with improved properties has attracted extensive research interest during past few years. If two components are mixed at nanometer level, they usually exhibit improved performance properties compared to conventional composites [16,17]. Blends of polymers and montmorillonite (clay) have been studied extensively because a small amount of well-dispersed clay layers in the polymer matrix can improve their mechanical and thermal properties. The inorganic layered silicate structure of the clay, however, does not permit it to disperse well in the organic polymer matrix and it is essential to pretreat the clay with appropriate surfactants [14,15]. Recently, a novel class of organic/inorganic hybrid material based on polyhedral oligomeric silsesquioxane (POSS) has been developed [18–20]. POSS is an inorganic  $Si_8O_{12}$  core and the core can be designed by attaching seven inert organic hydrocarbon groups and a unique functional group or eight functional groups that is able to undergo polymerization or crosslinking [21–26]. If these inorganic POSS particles are evenly distributed within the

<sup>\*</sup> Corresponding authors. Tel./fax: +886 3 5131512.

E-mail addresses: [kuosw@mail.nctu.edu.tw](mailto:kuosw@mail.nctu.edu.tw) (S.-W. Kuo), [changfc@mail.nctu.edu.tw](mailto:changfc@mail.nctu.edu.tw) (F.-C. Chang).

organic matrix at the nanometer scale (1–100 nm), they usually can dramatically improve their thermal stability [27] and mechanical strength. In contrast to the clay or conventional fillers, POSS have the advantages of being monodisperse molecular weight with well-defined structure, lower density, high-temperature stability, and containing no trace metals, and sizable interfacial interaction between composite particles and polymer segments. Each POSS compound may contain one or more reactive sites; therefore, it can be easily incorporated into common polymers. To improve the property of the material, the POSS can be introduced into the matrix with polymerizable groups. In our previous study, we have synthesized monofunctional benzoxazine-substituted POSS (BZ-POSS) incorporated into polybenzoxazine matrix by ring-opening polymerization [28]. The thermal properties of these hybrids are improved relative to those of the pure polybenzoxazine when analyzed by differential scanning calorimetry (DSC) and thermal gravimetric analysis (TGA). In this work, a multifunctional POSS bearing with eight benzoxazine groups (MBZ-POSS) was synthesized and copolymerized with other commercial benzoxazine monomers (Pa and Ba) via ring opening polymerization. These polybenzoxazine–POSS hybrid materials with small POSS amount result in noticeable thermal stability improvement confirmed by the DSC and TGA. Microstructure analyses of resulted hybrids were characterized by atomic force microscopy (AFM). The goal of this study is to develop a network architecture of the polybenzoxazine/POSS nanocomposites and to analyze the morphology–thermal properties relationships of the resulting organic–inorganic materials.

## 2. Experimental

### 2.1. Materials

Paraformaldehyde, phenol, and allylamine were purchased from Tokyo Kasei Kogyo Co., Japan. Platinum complex (Pt-dvs, 2 wt% Pt in xylene) was purchased from Aldrich, USA. Before use, the solution of the platinum complex was diluted 100-fold with xylene. Toluene was dried by distillation before use in the hydrosilylation reaction. Octakis(dimethylsiloxy)silsesquioxane ( $Q_8M_8^H$ ) containing eight hydro-silane groups was purchased from the Hybrid Plastics Co., USA. The benzoxazine monomers, Pa and Ba, were purchased from Shikoku Chemicals Co., Japan.

### 2.2. Characterizations

$^1H$  and  $^{13}C$  nuclear magnetic resonance (NMR) spectra were obtained at 300 MHz using a Bruker DPX-300 Spectrometer. Infrared spectroscopic measurements were performed using a Nicolet Avatar 320 FT-IR Spectrophotometer in the range  $4000$ – $400$   $cm^{-1}$  at a resolution of  $1.0$   $cm^{-1}$ . All sample preparations were performed under a continuous flow of nitrogen to ensure minimal oxidation or degradation of these samples. Molecular weights were determined by the gel-permeation chromatography (GPC)

using a SUPER CO-150 apparatus equipped with an LC gel column and an RI detector. Polystyrene samples were used as standards and THF was used as the eluent at a flow rate of 1 ml/min.

Thermal properties of the benzoxazine copolymers were characterized by DSC and TGA. DSC measurements were carried out with a DSC-910s instrument from TA Co., USA, at a scanning rate at  $10$   $^{\circ}C/min$ . The sample was heated at  $300$   $^{\circ}C$  for 1 min and then cooled down to  $30$   $^{\circ}C$  for 3 min. The sample was then reheated immediately to measure the glass transition temperature ( $T_g$ ) of the copolymer. TGA was carried out using a TA Instruments TGA 2050 Thermal Gravimetric Analyzer at a heating rate of  $10$   $^{\circ}C$  from room temperature to  $700$   $^{\circ}C$  under a continuous flow of nitrogen. The surface morphology was recorded using the ‘easyscan’ contact mode of an atomic force microscopy (AFM) system (Nanosurf AG). The spring constant of the cantilever was 5 N/m and the feedback loop bandwidth was 12 kHz. All images were recorded at room temperature.

### 2.3. Syntheses

#### 2.3.1. The vinyl-terminated benzoxazine (VP-a)

Allylamine (11.4 g, 0.2 mol) and phenol (18.8 g, 0.2 mol) were stirred for 10 min in an ice bath and then the paraformaldehyde (12 g, 0.4 mol) was added portion-wise over 10 min. After stirring for 30 min, the temperature was raised gradually up to  $90$   $^{\circ}C$  and maintained at that temperature under constant stirring for 3 h. The mixture was then cooled to room temperature and dissolved in ethyl ether (200 ml). The solution was washed several times with water and 3 N NaOH to remove any impurities and un-reacted monomers. The ethyl ether solution was then dried (sodium sulfate) and the product was recovered under vacuum at room temperature. The VP-a monomer can be further purified by distillation under reduced pressure. The product was obtained as a viscous light-yellow fluid (25.2 g, 68%). The structure of the VP-a was confirmed by  $^1H$  NMR,  $^{13}C$  NMR, FT-IR, and elemental analysis.

$^1H$  NMR (300 MHz,  $CDCl_3$ ): 6.75–7.13 (4H, aromatic CH), 4.85 ppm (2H,  $-N-CH_2-O-$ ), 3.96 ppm (2H,  $-N-CH_2-Ar$ ), 5.90 ppm (1H,  $-CH_2-CH-CH_2$ ), 5.24 ppm (2H,  $-CH-CH_2$ ), 3.4 ppm (2H,  $-N-CH_2-CH$ ).

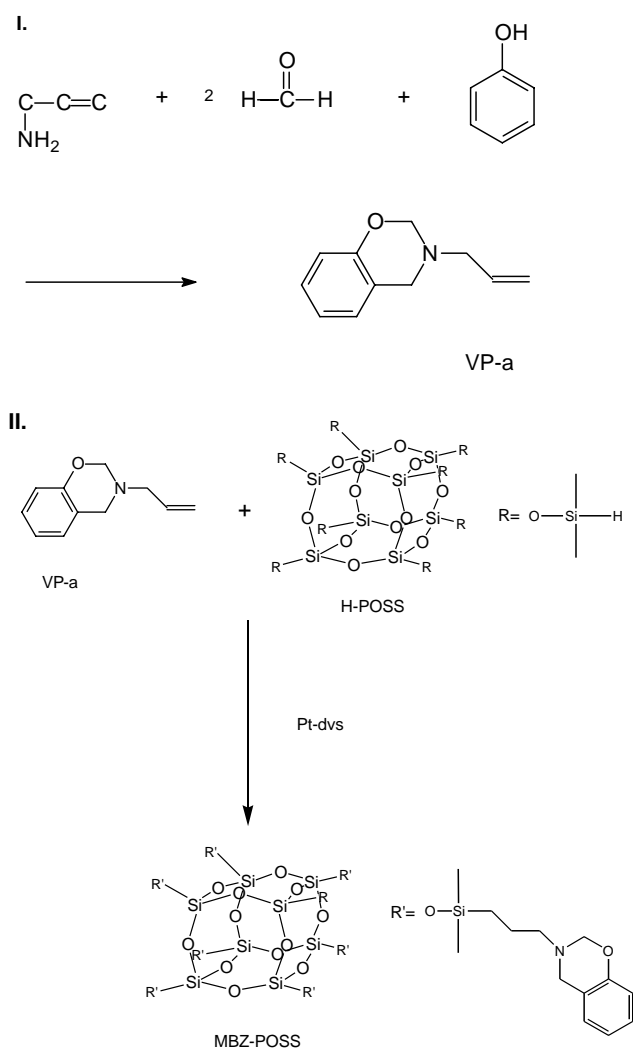
$^{13}C$  NMR: 81.54 ppm ( $-O-CH_2-N-$ ), 54.10 ( $-N-CH_2-Ar$ ), 127.25 ppm ( $-CH_2-CH=CH$ ), 118.41 ppm ( $-CH=CH_2$ ).

FT-IR (KBr,  $cm^{-1}$ ): 1024 (C–O–C), 922, 1490 (tri-substituted benzene ring), 1604 (aromatic C=C), 1644 (allyl C=C), 910 (=C–H).

Elemental analysis (% found):  $C_{11}H_{13}NO$ , C: 76.1, H: 7.41, N: 7.89 Calcd C: 75.4, H: 7.48, N: 7.95.

#### 2.3.2. The multifunctional POSS macromonomer (MBZ-POSS)

Both of the VP-a and  $Q_8M_8^H$  monomers are soluble in most common solvents, such as THF, toluene, chloroform, and acetone. The reaction was performed under  $N_2$  atmosphere using a dry toluene. The  $Q_8M_8^H$  was used without further purification. MBZ-POSS was prepared by the hydrosilylation



Scheme 1. Synthesis of the VP-a and preparation of the benzoxazine-functionalized-POSS (MBZ-POSS) via a hydrosilylation.

reaction of VP-a with  $Q_8M_8^H$ , as shown in Scheme 1. To start with, the platinum complex (Pt-dvs) was dissolved in xylene to form a 200 ppm solution before use. In a 100 ml flask,  $Q_8M_8^H$  (1.018 g, 1 mmol) and VP-a (1.75 g, 10 mmol) were dissolved in 50 ml dry toluene. 0.1 ml of Pt-dvs solution was then injected into the solution. The resultant solution was then heated at 70 °C with stirring for 24 h under nitrogen. After cooling the reaction mixture to room temperature, the triphenylphosphine (1 mg) was added. The solvent and the unreacted VP-a were evaporated under vacuum at 110 °C to give a pale yellow viscous liquid. The structure of the VP-a was confirmed by  $^1H$  NMR,  $^{13}C$  NMR, FT-IR, elemental analysis, and GPC. The molecular weight and their distribution of the MBZ-POSS is shown in Table 1. According to  $^1H$  NMR

analysis, the reaction generated product with 55% of the  $\beta$  adduct and 45%  $\alpha$  adduct.

$^1H$  NMR (300 MHz,  $CDCl_3$ ): 6.8–7.2 (32H, aromatic CH), 4.98 ppm (16H,  $-N-CH_2-O-$ ), 3.72 ppm (16H,  $-N-CH_2-Ar$ ), 2.25 ppm (8.8H,  $-CH_2-CH_2-N-$ ,  $\beta$ ), 2.14 ppm (3.6H,  $-CH(CH_3)-CH_2-N-$ ,  $\alpha$ ), 1.40 ppm (17.6H,  $Si-(CH_2)_2-CH_2-$ ,  $\beta$ ), 1.23 ppm (10.8H,  $Si-CHCH_3$ ,  $\alpha$ ), 0.05 (26.4H,  $(CH_3)_2-Si-CH_2$ ,  $\beta$ ), 0.16 (21.6H,  $(CH_3)_2-Si-CH$ ,  $\alpha$ ).

$^{13}C$  NMR: 82.33 ppm ( $-O-CH_2-N-$ ), 55.10 ( $-N-CH_2-Ar$ ), 48.92, 29.83, 21.87, 14.68 ppm, ( $-N-(CH_2)_x-Si$ ,  $\alpha$  and  $\beta$  adducts),  $-0.5$ ,  $0.5$  ppm ( $-O-Si-CH_3$ ,  $\beta$ ,  $\alpha$ ).

FT-IR (KBr,  $cm^{-1}$ ): 1260 ( $Si-CH_3$ ), 790, 1089 ( $Si-O-Si$ ), 1174 ( $Si-C$ ), 1024 ( $C-O-C$ ), 922, 1490 (trisubstituted benzene ring), 1604 (aromatic  $C=C$ ).

Elemental analysis (%), found):  $C_{104}H_{80}O_{28}N_8$ , C: 52.3, H: 5.70, N: 5.10 Calcd C: 51.6, H: 6.0, N: 4.9.

### 2.3.3. Preparation of polybenzoxazine/POSS hybrids

Pa type benzoxazine monomer (0.95 g) and MBZ-POSS (0.05 g) were dissolved in THF (10 ml) and stirred for 30 min at room temperature. The solution was poured onto an aluminum plate and then left for 6 h in open air to evaporate most of the THF. The coated plate was then transferred to an oven and heated at 100 °C for 2 h. The cast film was then cured in a stepwise manner at 180 and 200 °C for 3 h each and then postcured at 220 and 240 °C for 1 h each. The cured sample was transparent in a red-wine color with a thickness of ca. 0.2 mm. The procedures were repeated to prepare other hybrid materials by varying the amount of POSS (0, 2, and 10 wt%). Finally, the hybrid material was extracted for 24 h with THF under reflux in a Soxhlet apparatus for 24 h to remove any unreacted monomers. The Ba type polybenzoxazine and its POSS hybrids were prepared and recovered under similar conditions (Scheme 2).

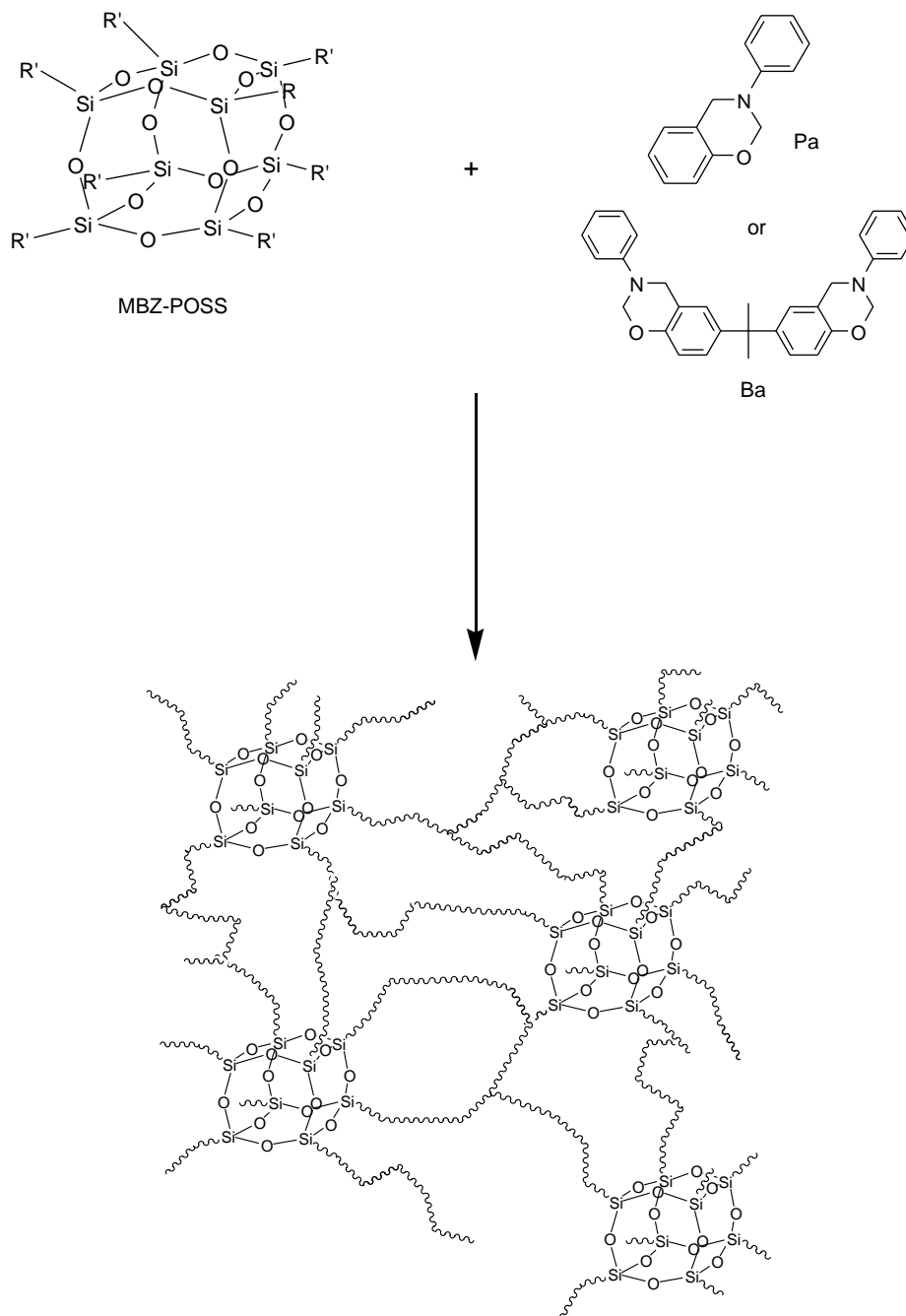
## 3. Results and discussion

### 3.1. NMR spectra of the vinyl-terminated benzoxazine (VP-a)

The vinyl-terminated benzoxazine (VP-a) was synthesized and used to prepare the novel POSS bearing eight benzoxazine groups. The presence of the vinyl group of the VP-a allows the hydrosilylation reaction to proceed under moderate conditions. Fig. 1(a) displays the  $^1H$  NMR spectrum of the vinyl-terminated benzoxazine (VP-a). The vinyl group is represented by two peaks at 5.2 and 5.9 ppm in a relative 2:1 ratio. We assign the peaks at 3.9 and 4.8 ppm to the protons of the methylene bridges of the benzoxazine ring. The protons between the vinyl group and the nitrogen atom appear as a signal at 3.4 ppm. The  $^{13}C$  NMR spectrum of the VP-a is presented in Fig. 1(b). The carbon atoms of the terminal olefin

Table 1  
Properties of MBZ-POSS

POSS (theory)	$M_n$ (g/mol)	$M_w$ (g/mol)	$M_w/M_n$	C (%)	H (%)	N (%)
MBZ-POSS	2465 (2418)	2514 (2418)	1.02 (1.00)	52.3 (51.6)	5.7 (6.0)	5.1 (4.9)



Scheme 2. Preparation and network structure of polybenzoxazine/POSS hybrids.

unit appear at 118 and 127 ppm. The characteristic carbon atoms of the benzoxazine ring are at 54 and 81 ppm. These  $^1\text{H}$  NMR and  $^{13}\text{C}$  NMR spectra confirm that the VP-a was indeed synthesized successfully.

### 3.2. FT-IR and NMR spectra of the multifunctional benzoxazine POSS (MBZ-POSS)

Fig. 2 shows the IR spectra of the MBZ-POSS samples measured during reaction. Aliphatic C–H stretching and bending peaks of the VP-a and the POSS are observed at below  $3000$  and  $1450\text{ cm}^{-1}$ . The IR spectrum of the POSS

clearly shows the symmetric stretching of Si–O–Si peak at  $1089\text{ cm}^{-1}$ . A peak for the spacer Si–CH<sub>3</sub> group is also observed at  $1260\text{ cm}^{-1}$ . There is an absence of Si–H peak at  $2139\text{ cm}^{-1}$ , which validates the structure of octafunctionalized POSS. The other characteristic absorption bands of the C–H bending from the vinyl group of the VP-a are assigned at  $910\text{ cm}^{-1}$ . By comparing in Fig. 2, the absorption band of the Si–H of Q<sub>8</sub>M<sub>8</sub><sup>H</sup> at  $2139\text{ cm}^{-1}$  is the result of total consumption after 12 h. In Fig. 3, the intensity of the Si–C band of the MBZ-POSS was increased at  $1174\text{ cm}^{-1}$  because of the increased new band of the synthetic benzoxazine-POSS spacer after the reaction. In addition, the stretching band of C–O–C at

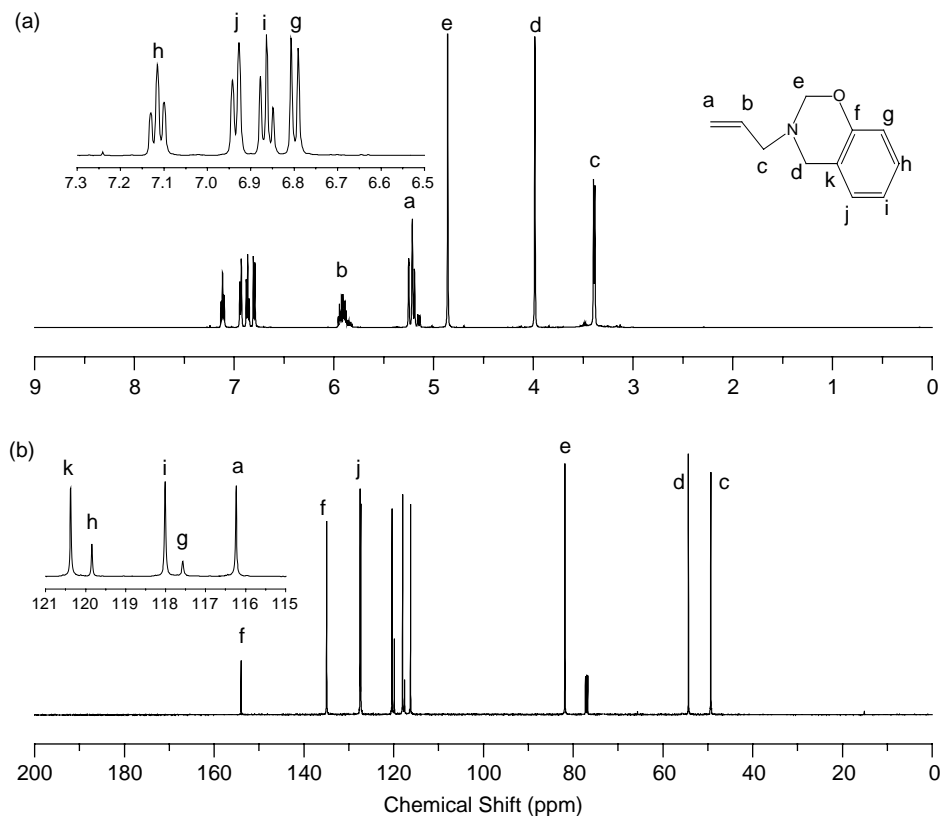


Fig. 1. (a)  $^1\text{H}$ , and (b)  $^{13}\text{C}$  NMR spectra of VP-a.

$1225\text{ cm}^{-1}$  of the oxazine ring and the 1,2,4-substitution of the benzene ring at  $922$  and  $1490\text{ cm}^{-1}$  were not consumed after a hydrosilylation reaction. It is suggesting that the ring-opening and other coupling reaction of the VP-a did not occur during this reaction. Moreover, the addition of the silane across the alkene can occur in both  $\alpha$  and  $\beta$  modes. The formation of  $\alpha$  and  $\beta$  adducts of MBZ-POSS was observed in both the  $^1\text{H}$  and  $^{13}\text{C}$  NMR spectra, as shown in Fig. 4(a) and (b). The proportion of the  $\beta$ -adduct (55%) of MBZ-POSS was higher than that of the  $\alpha$ -adduct (45%) due to the reaction mechanism and steric hindrance, which was similar to other silsesquioxane

derivatives reported in the literature [29–31]. Both the NMR and FT-IR results suggest that  $\text{Q}_8\text{M}_8^{\text{H}}$  was fully functionalized by VP-a through a hydrosilylation reaction. It is important for  $\text{Q}_8\text{M}_8^{\text{H}}$  to be fully functionalized because any remaining Si–H would be unstable and chemically reactive to undesired reaction.

Table 1 summarized results from elemental analysis (EA) and GPC. The element contents of MBZ-POSS from the EA are in a good agreement with the theoretical values. GPC was used in conjunction with molecular weight sensitive detection systems to determine absolute molecular weights and the molecular weight distribution. The number average molecular

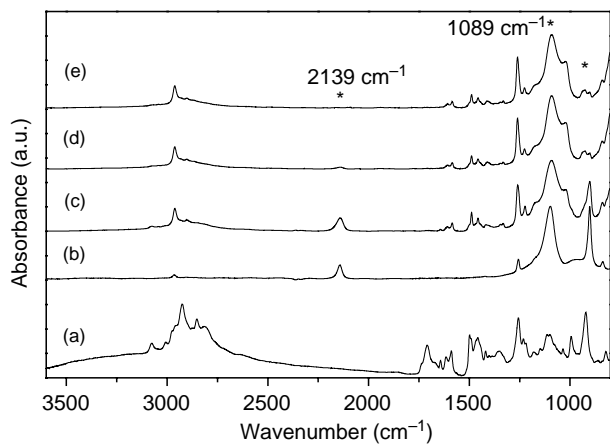


Fig. 2. IR spectra of MBZ-POSS recorded at different reaction time (a) VP-a monomer (b) pure  $\text{Q}_8\text{M}_8^{\text{H}}$  POSS (c) unreacted POSS with 10 equiv. VP-a monomers (d) reacted for 8 h and (e) reacted for 12 h.

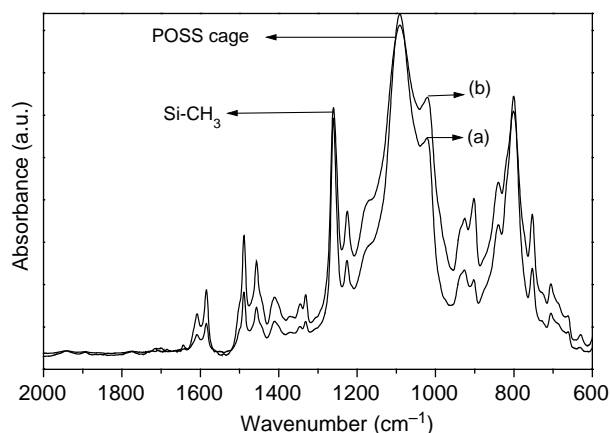


Fig. 3. IR spectra recorded in the  $600\text{--}2000\text{ cm}^{-1}$  region at (a) unreacted POSS with 10 equiv. VP-a monomers (b) reacted for 12 h.

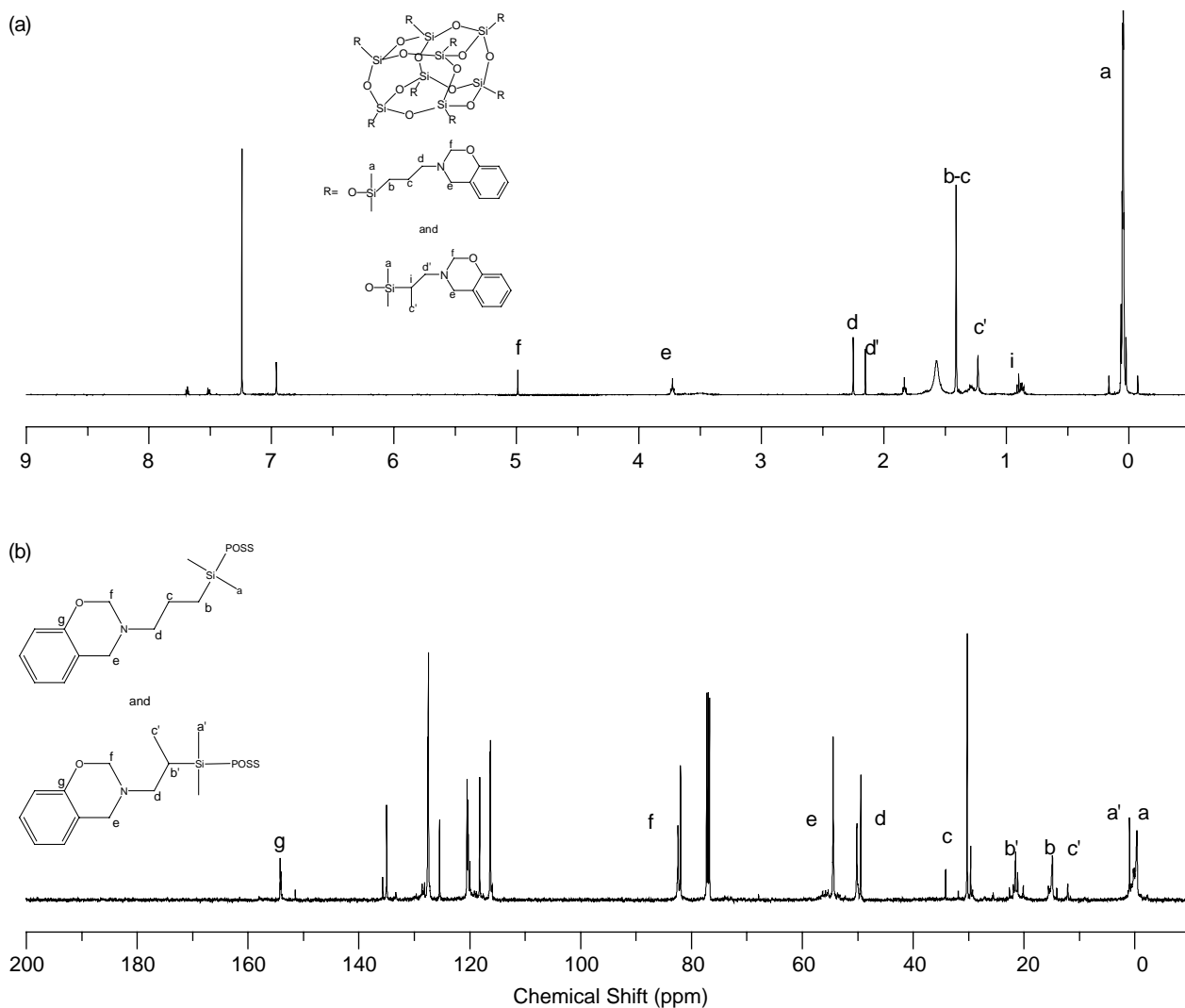


Fig. 4. (a)  $^1\text{H}$ , and (b)  $^{13}\text{C}$  NMR spectra of the MBZ-POSS.

weight ( $M_n$ ) and polydispersity indices (PDI) can be used to evaluate the molecular weight distributions. The  $M_n$  and PDI estimated from GPC are 2250 and 1.02, respectively. The pure MBZ-POSS gave very narrow PDI, which would normally suggest a very uniform molecular weight distribution for GPC calibration standards. The lower PDI indicates such spherical molecular probably has similar hydrodynamic radii due to their rigid structure.

### 3.3. Preparation of the polybenzoxazine/POSS hybrids and their thermal properties

Polybenzoxazine/POSS nanocomposite materials possess many desirable properties such as low moisture absorption, high solvent resistance, and improved thermal stability, and certain low dielectric properties [32,33]. We have prepared the polybenzoxazine/POSS composites as indicated in Scheme 2. Both the benzoxazine monomers (Pa and Ba) and MBZ-POSS are soluble in THF or acetone. These readily processible monomers can be polymerized at 180 °C, which are used to synthesize hybrid polymers containing different POSS contents

via a ring-opening polymerization. Tables 2 and 3 summarize components of these hybrids. The mixture were processed onto an aluminum plate to evaporate the solvent and then cured at 180 and 200 °C for 3 h each in an air oven. The samples were then postcured at 220 °C for 1 h and all the cured samples were transparent with dark red color (ca. 0.2 mm). At higher POSS contents (15 and 20 wt%), the prepared materials were cloudy and friable through the similar condition. This result indicates that the MBZ-POSS has an inorganic silsesquioxane core that may aggregate seriously during the polymerization. Tables 2 and 3 summarize the thermal characterizations of the

Table 2  
Summary of the thermal properties of Pa-POSS nanocomposites

Sample	MBZ-POSS in feed		$T_g$ (°C)	5 wt% Loss temperature (°C in $\text{N}_2$ )	Char yield in $\text{N}_2$ (wt%, 700 °C)
	wt%	mol			
Pa-0P	0	0	138	308	44
Pa-2P	2	0.0008	181	322	62
Pa-5P	5	0.0020	208	358	68
Pa-10P	10	0.0041	185	360	71

Table 3  
Summary of the thermal properties of Ba-POSS nanocomposites

Sample	MBZ-POSS in feed		$T_g$ (°C)	5 wt% Loss temperature (°C, in $N_2$ )	Char yield in $N_2$ (wt%, 700 °C)
	wt%	mol			
Ba-0P	0	0	162	350	38
Ba-2P	2	0.0008	174	354	43
Ba-5P	5	0.0020	192	362	51
Ba-10P	10	0.0041	177	370	65

polybenzoxazine/POSS hybrids. In these organic–inorganic hybrid materials, the cubic silsesquioxane core is rigid and the eight curable benzoxazine groups are appended to the silsesquioxane core via –Si–O– linkages. In a network structure, the  $T_g$  relates directly to the cross-linking density [34]. The  $T_g$ s increased upon increasing the MBZ-POSS content from 0 to 5 wt%, as indicated in Fig. 5(a) and (b). It also confirms that the MBZ-POSS acts as a multifunctional curing agent and the MBZ-POSS at lower content is expected to be distributed on a nanometer scale within the polymer matrix. Strong interfacial interaction like the ones leading to  $T_g$  changes close to hard surfaces and rigid POSS particles hinder the mobility of the polymer chains and result in higher  $T_g$  as would be expected [35,36]. When the MBZ-POSS content is increased to 10 wt%, the resulted  $T_g$  does not increase further and it actually decreases comparing to the 5 wt%. As a result, the cross-linking density of the hybrid tends to be reduced. It is well-known that  $T_g$  of a crosslinked network structure would decrease with decreasing of its cross-linking density. Below 5 wt%, the MBZ-POSS is expected to be distributed within the polymer matrix on a nanometer scale. When increasing the MBZ-POSS content to 10 wt%, in both the Pa and Ba types of hybrid polymers, the glass transition temperature were not

increased substantially and the blend films were become cloudy, which suggests that the MBZ-POSS units probably aggregate at higher content. When the MBZ-POSS content up to 10 wt%, however, the aggregated MBZ-POSS units cause macro-phase separation, which reduces its overall effectiveness in hindering polymer movement [35,36].

The thermal stabilities under nitrogen of the polybenzoxazine/POSS composites are given in Fig. 6(a) and (b). In a comparison of the thermal stabilities, 5 wt% weight loss temperature is used as a standard. A gradual increase in the decomposition temperature ( $T_d$ ) of the Ba-POSS or Pa-POSS composite was observed upon increasing POSS content from 0 to 10 wt%. The difference in thermal stability of the decomposition temperature may be construed as an effect of creating nanocomposite. In nanocomposite material, tether thermal motion is restricted thereby reducing the organic decomposition pathways accessible to the tether. The inorganic component (POSS) provides additional heat capacity thereby stabilizing the materials against thermal decomposition [37,38]. Char yielding, another indicator of thermal stability also increases upon the increasing (POSS) content of these hybrid materials in both monomers. For these hybrids, increasing the POSS content in the composite is expected to improve its thermal properties. The results indicate that the thermal stability of polybenzoxazines is improved through network structures and the inorganic silsesquioxane. In addition, the microstructure feature are useful to explain the thermal property changes ( $T_g$  and  $T_d$ ) detected by DSC and TGA [39]. For these polybenzoxazine/POSS hybrids, increasing the MBZ-POSS content leads to various morphological, and hence, microstructural analysis is useful to explain this phenomena.

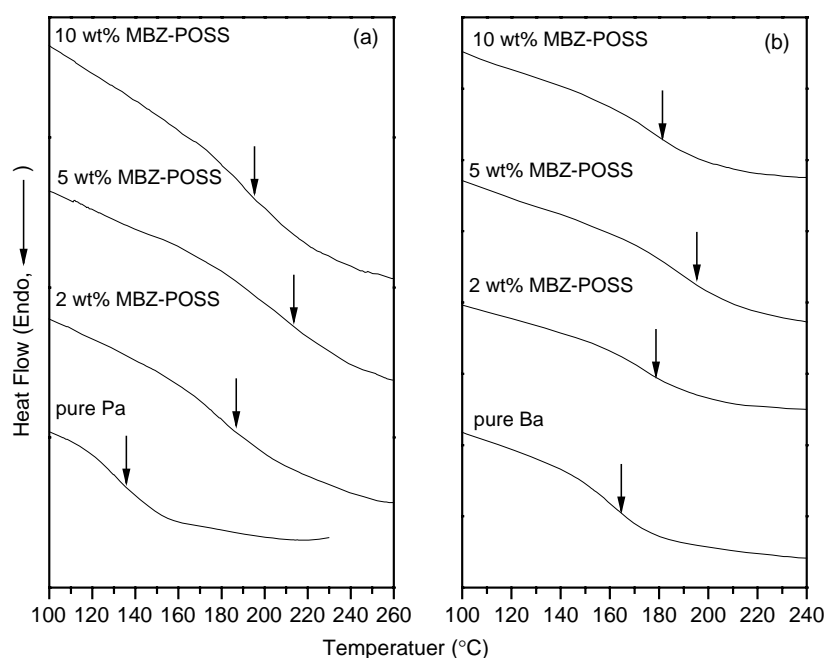


Fig. 5. DSC thermograms of polymeric (a) Pa, and (b) Ba having varying MBZ-POSS contents. (the arrow indicates the temperature of  $T_g$ ).

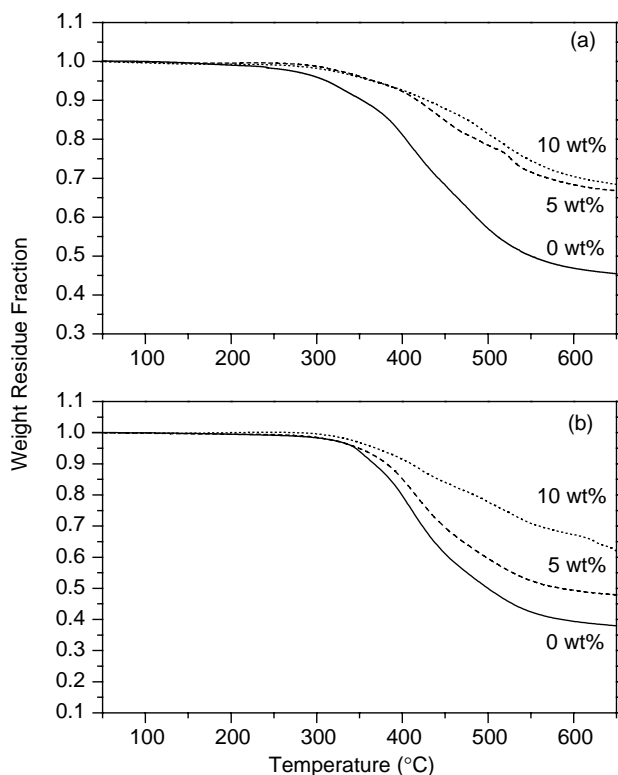


Fig. 6. TGA thermograms of (a) Pa, and (b) Ba type polybenzoxazine hybrids having varying MBZ-POSS contents.

### 3.4. Microstructural analysis

Surface analysis of polybenzoxazine/POSS composites were characterized by AFM. Fig. 7(a)–(f) displays the AFM images of hybrids having various polybenzoxazine/POSS ratios. The heterogeneous material showed the presence of different domains. Rough areas are POSS rich domains and smooth

areas are polybenzoxazine rich regions. In Fig. 7(a)–(d), we observe that the degree of roughness of the Pa type polybenzoxazine/POSS hybrid films increases upon increasing the POSS content. These POSS aggregation in larger scales occur at higher POSS contents. The reason of the heterogeneous phase separation may be the less dispersive of the POSS with benzoxazine species and the homopolymerization of MBZ-POSS, which tends to aggregate. This phase separation occurred when adding POSS to the benzoxazine monomers and was fixed by the polymerization reaction. By comparing Fig. 7(c) and (e), the domain size of the POSS/Ba blend is significantly greater than that of the POSS/Pa blend. At the same level of MBZ-POSS content (5 wt%), the POSS/Ba blend exhibits much more major aggregation than does the POSS/Pa blend. Serious aggregation of POSS occurs in the Ba type polybenzoxazine matrix because of the incompatibility of the inorganic POSS units. When the polymerization begins, these monomer units tend to react with other monomers in their vicinity, implying that those clustered MBZ-POSS monomers have a greater opportunity to react with each other formed MBZ-POSS aggregates that are separated from the polybenzoxazine matrix. In the course of the formation of the polybenzoxazine/POSS network, POSS was separated from the polybenzoxazine rich region, leading to POSS rich domains in the range of 50–1000 nm.

### 4. Conclusions

We have successfully synthesized a novel octafunctionalized POSS (MBZ-POSS) from VP-a and  $Q_8M_8^H$  by a platinum complex catalyzed hydrosilylation. The MBZ-POSS possesses a cross-linking unit that is able to undergo polymerization with other benzoxazine monomers, which allowed a new type of polybenzoxazine–POSS composite to be prepared. We prepared

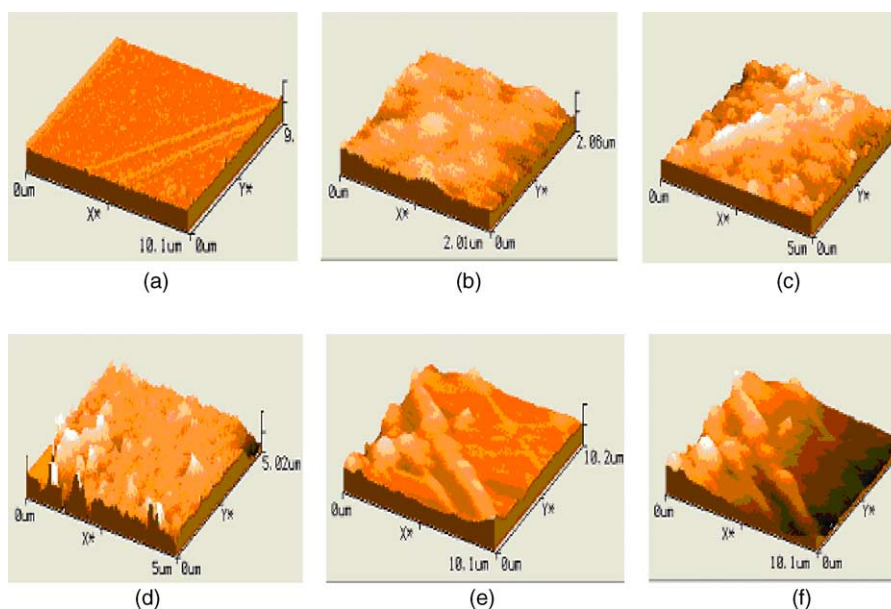


Fig. 7. AFM analysis of polybenzoxazine/POSS hybrid materials (a) pure Pa type polybenzoxazine, and (b) 2 wt% MBZ-POSS content, and (c) 5 wt% MBZ-POSS content, and (d) 10 wt% MBZ-POSS content. (e) Ba type polybenzoxazine having 5 wt% MBZ-POSS, and (f) 10 wt% MBZ-POSS content.



polybenzoxazine/POSS composites having various POSS contents and examined their thermal properties by DSC and TGA. Incorporation of MBZ-POSS into the polybenzoxazine could significantly enhance the thermal stability. Some of this can be explained by higher cross-linking densities resulting from the presence of the POSS-modified polybenzoxazine network. The dispersion between the MBZ-POSS and polybenzoxazine on a nanometer scale is only at low POSS content. Higher MBZ-POSS content resulted in the hybrids displaying apparently higher glass transition and thermal decomposition temperatures than that of the neat polybenzoxazine. The glass transition and decomposition temperatures of these nanocomposites are improved by incorporating the MBZ-POSS either the Ba or Pa type polybenzoxazine. However, the  $T_g$  values of POSS/polybenzoxazine hybrids with 10 wt% POSS content is lower than that of 5 wt% POSS inside probably due to hindrance of benzoxazines cross-link caused by hard POSS-rich particles resulting from phase separation. The concept arising from these results is that a phase separation process may take place when employing a POSS that are not compatible with the polybenzoxazine. This led to a macrophase separation (in a micrometer scale) into benzoxazine-rich and POSS-rich regions at a higher POSS content (10 wt%), due to the lack of compatibility between the organic resin and inorganic silsesquioxane and the homopolymerization of MBZ-POSS. This is an agreement of nanocomposites with results reported in this work for these polybenzoxazine modified with a small amount of multifunctional POSS. The in situ generation of a reinforced polymer might have practical application.

### Acknowledgements

This work was supported financially by the National Science Council, Taiwan, under contract No. NCS-94-2216-E-009-002.

### References

- [1] Burke W. J Am Chem Soc 1954;76:1677.
- [2] Burke W. J Org Chem 1949;71:109.
- [3] Ning X, Ishida H. J Polym Sci, Part A: Polym Chem 1994;32:1121.
- [4] Higginbottom HP. US Patent 1985, 4501864.
- [5] Su YC, Chang FC. Polymer 2003;44:7989.
- [6] Agag T, Takeichi T. Macromolecules 2001;34:7257.
- [7] Kim HJ, Brunoyska ZB, Ishida H. Polymer 1999;40:1815.
- [8] Agag T, Takeichi T. Macromolecules 2001;34:7257.
- [9] Kim HJ, Brunoyska ZB, Ishida H. Polymer 1999;40:6565.
- [10] Rimdusit S, Ishida H. Polymer 2000;41:7941.
- [11] Takeichi T, Guo Y, Agag T. J Polym Sci, Polym, Part A: Chem 2000; 38:4165.
- [12] Takeichi T, Guo Y. Polym J 2001;33:437.
- [13] Su YC, Kuo SW, Xu HY, Chang FC. Polymer 2003;44:2187.
- [14] Agag T, Takeichi T. Polymer 2000;41:7083.
- [15] Takeichi T, Agag T. Polymer 2002;43:45.
- [16] Mark JE, Lee CY-C, Bianconi PA, editors. Hybrid organic–inorganic composites. ACS symposium series 585. Washington, DC: American Chemical Society; 1995.
- [17] Miller B. Plast Formulating Compounding 1997;3:30.
- [18] Fina A, Tabuani D, Frache A, Camino G. Polymer 2005;46:7855.
- [19] Ricco L, Russo S, Monticelli O, Bordo M, Bellucci F. Polymer 2005; 46:6810.
- [20] Kopesky ET, Haddad T, Mckinley GH, Cohen RE. Polymer 2005; 46:4743.
- [21] Sellinger A, Laine RM. Macromolecules 1996;29:2327.
- [22] Lichtenhan JD, Otonari YA, Carr MJ. Macromolecules 1995;28:8435.
- [23] Zheng L, Farris RJ. J Polym Sci, Polym Chem Ed 2001;39:2920.
- [24] Lee A, Lichtenhan JD. Macromolecules 1998;31:4970.
- [25] Haddad TS, Lichtenhan JD. Macromolecules 1996;29:7302.
- [26] Lee YJ, Huang JM, Kuo SW, Chen JK, Chang FC. Polymer 2004; 46:2320.
- [27] Xu HY, Kuo SW, Lee JS, Chang FC. Polymer 2002;(43):5117.
- [28] Lee YJ, Kuo SW, Su YC, Chen JK, Tu CW, Chang FC. Polymer 2004;45:6321.
- [29] Ojima I. In: Patai S, Rappoport S, editors. The chemistry of organic silicon compounds. New York: Wiley; 1989.
- [30] Chalk AJ, Harrod JF. J Am Chem Soc 1965;87:16.
- [31] Takeuchi R, Yasue H. Organometallics 1996;15:2098.
- [32] Lee YJ, Huang JM, Kuo SW, Lu JS, Chang FC. Polymer 2005;46:173.
- [33] Lee YJ, Huang JM, Kuo SW, Chang FC. Polymer 2005;46:10056.
- [34] Kim KM, Keum DK, Chujo Y. Macromolecules 2003;36:867.
- [35] Choi J, Yee AF, Laine RM. Macromolecules 2003;36:5666.
- [36] Li GZ, Wang L, Toghiani H, Tyrone L, Koyama K, Pittman Jr CU. Macromolecules 2001;34:8686.
- [37] Choi J, Kim SG, Laine RM. Macromolecules 2004;37:99.
- [38] Choi J, Kim SG, Laine RM. Macromolecules 2003;15:3365.
- [39] Maria JA, Barral L, Fasce DP, Williams RJJ. Macromolecules 2003; 36:3135.